NeuroImage: Clinical 25 (2020) 102113

Contents lists available at ScienceDirect

NeuroImage: Clinical

journal homepage: www.elsevier.com/locate/ynicl

Hippocampal [^{18}F]flortaucipir BP_{ND} corrected for possible spill-in of the choroid plexus retains strong clinico-pathological relationships

Emma E Wolters[a,b,*], Rik Ossenkoppele[b,c], Sandeep SV Golla[a], Sander CJ Verfaillie[a], Tessa Timmers[a,b], Denise Visser[a], Hayel Tuncel[a], Emma M Coomans[a], Albert D Windhorst[a], Philip Scheltens[b], Wiesje M van der Flier[b,d], Ronald Boellaard[a], Bart NM van Berckel[a]

[a] Department of Radiology and Nuclear Medicine, Amsterdam Neuroscience, Vrije Universiteit Amsterdam, Amsterdam UMC, location VUmc, PO Box 7057, 1007 MB Amsterdam, the Netherlands
[b] Alzheimer Center Amsterdam, Department of Neurology, Amsterdam Neuroscience, Vrije Universiteit Amsterdam, Amsterdam UMC, Amsterdam, the Netherlands
[c] Clinical Memory Research Unit, Lund University, Lund, Sweden
[d] Department of Epidemiology and Biostatistics, Vrije Universiteit Amsterdam, Amsterdam UMC, Amsterdam, the Netherlands

ARTICLE INFO

Keywords:
[^{18}F]flortaucipir PET Quantifcation
Hippocampus Off-target

ABSTRACT

Background: Off-target [^{18}F]flortaucipir (tau) PET binding in the choroid plexus causes spill-in into the nearby hippocampus, which may influence the correlation between [^{18}F]flortaucipir binding and measures of cognition. Previously, we showed that partial volume correction (combination of Van Cittert iterative deconvolution and HYPR denoising; PVC HDH) and manually eroding the hippocampus resulted in a significant decrease of the choroid plexus spill-in. In this study, we compared three different approaches for the quantification of hippocampal [^{18}F]flortaucipir signal using a semi-automated technique, and assessed correlations with cognitive performance across methods.

Methods: Dynamic 130 min [^{18}F]flortaucipir PET scans were performed in 109 subjects (45 cognitively normal subjects (CN) and 64 mild cognitive impairment/Alzheimer's disease (AD) dementia patients. We extracted hippocampal binding potential (BP_{ND}) using receptor parametric mapping with cerebellar grey matter as reference region. PVC HDH was performed. Based on our previous study in which we manually eroded 40% ± 10% of voxels of the hippocampus, three hippocampal volumes-of-interest (VOIs) were generated: a non-optimized 100% hippocampal VOI [100%], and combining HDH with eroding a percentage of the highest hippocampus BP_{ND} voxels (i.e. lowering spill-in) resulting in optimized 50%[50%HDH] and 40%[40%HDH] hippocampal VOIs. Cognitive performance was assessed with the Mini-Mental State Examination (MMSE) and Rey auditory verbal learning delayed recall. We performed receiver operating characteristic analyses to investigate which method could best discriminate MCI/AD from controls. Subsequently, we performed linear regressions to investigate associations between the hippocampal [^{18}F]flortaucipir BP_{ND} VOIs and MMSE/delayed recall adjusted for age, sex and education.

Results: We found higher hippocampal [^{18}F]flortaucipir BP_{ND} in MCI/AD patients ($BP_{ND100\%} = 0.27 \pm 0.15$) compared to CN ($BP_{ND100\%} = 0.07 \pm 0.13$) and all methods showed comparable discriminative effects ($AUC_{100\%} = 0.85$[CI = 0.78–0.93]; $AUC_{50\%HDH} = 0.84$[CI = 0.74–0.92]; $AUC_{40\%HDH} = 0.83$[CI = 0.74–0.92]). Across groups, higher [^{18}F]flortaucipir BP_{ND} was related to lower scores on MMSE (standardized $\beta_{100\%} = -0.38$[CI = -0.57 − 0.20]; $\beta_{50\%HDH} = -0.37$[CI = -0.54 − 0.19]; $\beta_{40\%HDH} = -0.35$[CI = -0.53 − 0.17], all $p < 0.001$) and delayed recall (standardized $\beta_{100\%} = -0.64$[CI = -0.79 − 0.49]; $\beta_{50\%HDH} = -0.61$[CI = -0.76 − 0.46]; $\beta_{40\%HDH} = -0.59$[CI = -0.75 − 0.44]; all $p < 0.001$), with comparable effect sizes for all hippocampal VOIs.

Conclusions: Hippocampal tau load measured with [^{18}F]flortaucipir PET is strongly associated with cognitive function. Both discrimination between diagnostic groups and associations between hippocampal [^{18}F]flortaucipir BP_{ND} and memory were comparable for all methods. The non-optimized 100% hippocampal VOI may be sufficient for clinical interpretation. However, proper correction for choroid plexus spillover and may be required in case of smaller effect sizes between subject groups or for longitudinal studies.

* Corresponding author at: Department of Radiology and Nuclear Medicine, Amsterdam Neuroscience, Vrije Universiteit Amsterdam, Amsterdam UMC, location VUmc, PO Box 7057, 1007 MB Amsterdam, the Netherlands.
E-mail address: ee.wolters@amsterdamumc.nl (E.E. Wolters).

https://doi.org/10.1016/j.nicl.2019.102113
Received 24 June 2019; Received in revised form 22 November 2019; Accepted 1 December 2019
Available online 02 December 2019

1. Introduction

Alzheimer's disease (AD) is neuropathologically characterized by extracellular amyloid plaques (Aβ) and intracellular tau neurofibrillary tangles (Nelson et al., 2009; Braak and Braak, 1991). The advent of the positron emission tomography (PET) tracer [^{18}F]flortaucipir([^{18}F]AV-1451) has made it possible to image tau pathology in vivo (Marquie et al., 2015). [^{18}F]Flortaucipir binds with high affinity to paired helical filaments (PHF) of tau, with strong correlations to the clinical diagnosis of AD and degree of cognitive impairment (Ossenkoppele et al., 2016; Johnson et al., 2016; Scholl et al., 2016; Pontecorvo et al., 2017; Ossenkoppele et al., 2018). However, the tracer is also characterized by off-target binding in the basal ganglia, thalamus and choroid plexus (Marquie et al., 2015; Vermeiren et al., 2018; Lowe et al., 2016). Off-target binding in the choroid plexus may cause spill-in to the anatomical nearby hippocampus. This spill-in effect may artificially increase hippocampal [^{18}F]flortaucipir signal leading to an inaccurate quantification of hippocampal tau load. Indeed, choroid plexus spill-in may partly explain the strong associations between the choroid plexus and hippocampus (Scholl et al., 2016; Lee et al., 2018; Wang et al., 2016; Wolters et al., 2018). This is potentially problematic as the hippocampus is among the earliest regions affected by tau pathology and accurate assessment of this early tau accumulation is of utmost importance in our understanding of the natural time course of AD (Price and Morris, 1999).

Former studies investigating specifically the role of hippocampal tau in relation to the clinical diagnosis of AD have generated inconsistent results. Some studies, using semi-quantitative techniques, accurately distinguished AD patients from cognitive normal participants with hippocampal [^{18}F]flortaucipir uptake (Wang et al., 2016), while others did not (Johnson et al., 2016; Pontecorvo et al., 2017). Eroding voxels of the hippocampus (Wolters et al., 2018), various partial volume correction (PVC) methods (Scholl et al., 2016; Wolters et al., 2018; Wang et al., 2016) and linear regression approaches (Lee et al., 2018; Wang et al., 2016) have been proposed to reduce the spill-in effect of the choroid plexus[13]. These methods resulted in a decreased association between hippocampal and choroid plexus tracer uptake, presumably due to lowering the spill-in effects (Scholl et al., 2016; Lee et al., 2018; Wang et al., 2016; Wolters et al., 2018). However, limited evidence is available regarding the effects of an optimized hippocampal [^{18}F]flortaucipir signal on the relationships between tau pathology and cognition (Lee et al., 2018).

Here we build upon previous work (Wolters et al., 2018) in which we used a PVC method that combines Van Cittert iterative deconvolution with highly constrained back projection (HDH). This PET-only based PVC method results in a better quantification of the dynamic PET signal (Golla et al., 2017). The use of PVC HDH with an manually eroded hippocampal volume-of-interest (VOI) effectively reduced the spill in from the choroid plexus and improved the quantitative accuracy of the hippocampal tau load (Wolters et al., 2018). However, this technique is time consuming and impractical due to the manually eroding of the hippocampus. In addition, the technique has not yet been validated using clinical parameters of AD, such as cognitive measures. This additional step is important because using PVC could potentially increase noise (Golla et al., 2017) and could blur the associations with clinical correlates of AD. Clinical validation of the HDH PVC method is therefore important, especially in AD where atrophy plays an important role and thus partial volume effects are to be expected.

As such, the purpose of the present study was to compare three different semi-automatic hippocampal VOIs and examine which hippocampal VOI showed the best correlation with cognitive performance. We hypothesised that the improved quantification of hippocampal tau load, using both PVC and an eroded hippocampus volumes (i.e. reducing spill-in effects), would provide higher accuracy for distinguishing AD from controls and would be most strongly related to cognition in a memory clinic population.

2. Methods

2.1. Participants

We included 109 subjects, 45 cognitively normal individuals with subjective cognitive decline (SCD) from the SCIENCe project (Slot et al., 2018) and 64 patients with cognitive impairment from the Amsterdam Dementia Cohort (van der Flier et al., 2014, 2018). Among the 64 patients with cognitive impairment, nine patients were diagnosed with mild cognitive impairment (MCI) due to Alzheimer's disease(AD) (Albert et al., 2011) and 55 with AD dementia (McKhann et al., 2011). All subjects visited the Alzheimer Center Amsterdam, Amsterdam UMC, location VUmc, for an extensive dementia screening. The standardized work up consists of a clinical evaluation by a neurologist, including physical examination, neuropsychological investigation, brain magnetic resonance imaging (MRI) and a lumbar puncture. A clinical diagnosis was established by a multidisciplinary consensus meeting (van der Flier et al., 2014, 2018) and all AD/MCI patients had evidence for amyloid pathology determined by either an abnormal amyloid PET scan (n = 24) by visual read (Seibyl et al., 2016; Zwan et al., 2014) and/or an AD-like CSF profile (n = 59) (Tijms et al., 2018), or both CSF and PET(n = 20). Cognitively normal individuals with evidence of substantial Aβ pathology after visual reading of [^{18}F]florbetapir Aß-PET scans $SUVr_{50-70}$ min (Golla et al., 2018), were classified as amyloid positive subjects. In all cases with both CSF and PET data available, biomarkers were concordant. The study protocol was approved by the Medical Ethics Review Committee of the Amsterdam UMC VU Medical center. All patients provided written informed consent.

2.2. Image acquisition

Dynamic 130 min [^{18}F]flortaucipir PET scan were acquired on a Philips Ingenuity TF-64 PET/CT scanner. The scanning protocol consisted of two dynamic PET scans of 60 and 50 min respectively, with a 20 min break in between (Wolters et al., 2018; Golla et al., 2017). The first 60 min dynamic scan started simultaneously with a bolus injection 237 ± 13 MBq (injected mass 1.14 ± 0.84 μg) of [^{18}F]flortaucipir. The second PET scan was co-registered to the first dynamic PET scan using Vinci software (Vollmar et al., 2002). PET list mode data were rebinned into a total of 29 frames (1 × 15, 3 × 5, 3 × 10, 4 × 60, 2 × 150, 2 × 300, 4 × 600 and 10 × 300 s) and reconstructed using 3D RAMLA with a matrix size of 128 × 128 × 90 and a final voxel size of 2 × 2 × 2 mm^3, including standard corrections for dead time, decay, attenuation, randoms and scatter.

All subjects also underwent a 3D-T1 weighted sequence on a 3.0 Tesla MRI scanner (Ingenuity TF PET/MR, Philips Medical Systems, Best, The Netherlands), and these images were co-registered to the averaged images (frame 8 – 29) of the PET scan. The time lag between MR and PET scan was maximal 6 months (1.4 ± 2.2 months) for MCI/AD patients and 12 months (−3.0 ± 6.8 months) for cognitively normal individuals. The hippocampal volume of interest (VOI, Hammers template (Hammers et al., 2003)) was subsequently defined on the MR images and superimposed on the PET scan using PVElab (Svarer et al., 2005). Hippocampal binding potential (BP_{ND}) was generated using a basis function approach of the simplified reference method, i.e. receptor parametric mapping (RPM) with whole cerebellar gray matter as a reference region (Golla et al., 2017, 2018; Nelson et al., 2009).In addition, using the Hammers template (Hammers et al., 2003), we constructed a ROI consisting of all cortical structures to obtain a measurement of global [^{18}F]flortaucipir uptake. In our previous paper (Wolters et al., 2018) we showed that quantification of hippocampal tau load can be improved with the combination of PVC HDH and manually eroded hippocampus volumes which resulted in reduced spill in of the choroid plexus into the hippocampus. Approximately 40% ± 10% of the total hippocampal voxels were removed for the most optimal eroded hippocampus VOI (Wolters et al., 2018). For this

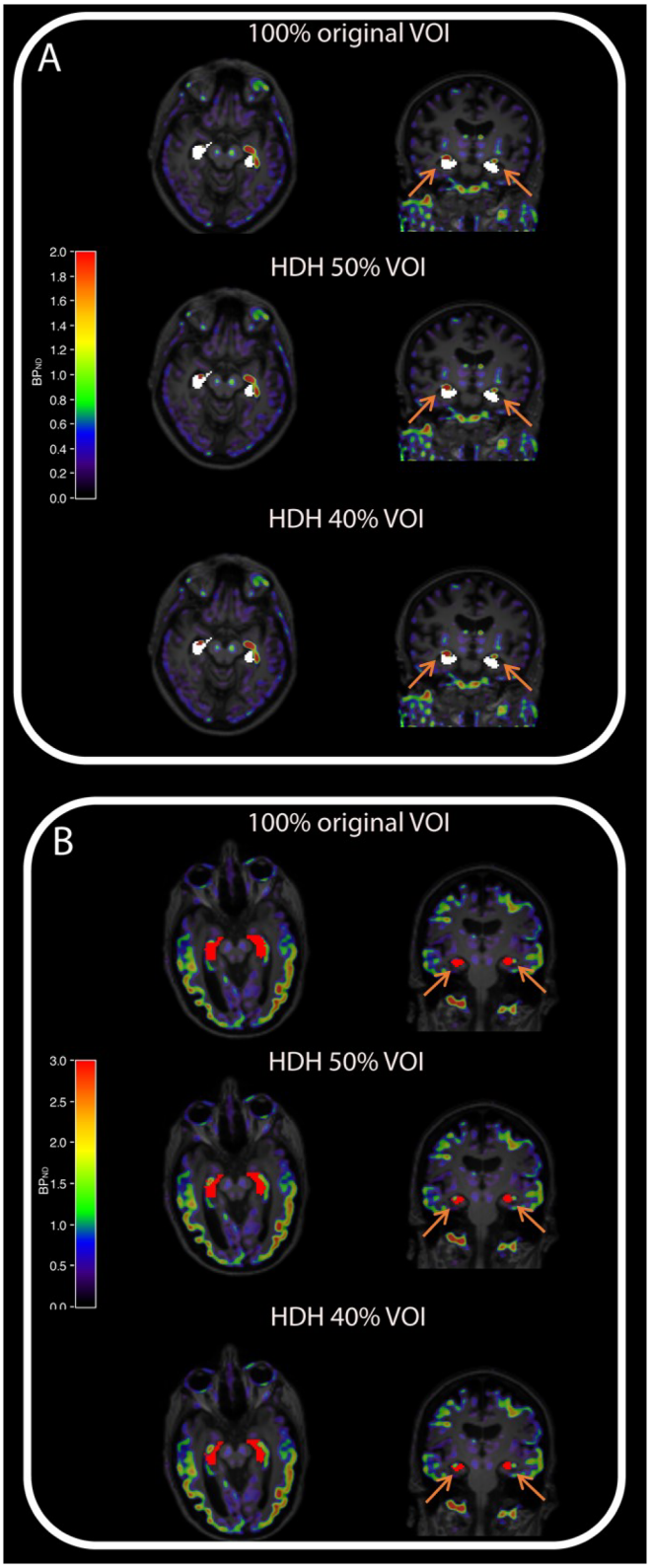

Fig. 1. RPM BP_{ND} PET images with examples of the different hippocampal VOIs (100% original, HDH 50%, HDH 40%) for a cognitively normal participant(A) and MCI/AD patient (B). For the cognitively normal participant the hippocampal VOI is depicted in white and high choroid plexus binding in red (as depicted by the orange arrow). For the MCI/ AD patients the hippocampal VOI is depicted in red and high choroid plexus binding in green (as depicted by the orang arrow). (For interpretation of the references to color in this figure legend, the reader is referred to the web version of this article.)

reason, in the present study, three hippocampal volumes of interest (VOIs) were generated: a non- optimized 100% hippocampal VOI [100%] (Hammers atlas-based), and automatically eroding a percentage of the highest hippocampus BP_{ND} voxels (i.e. lowering spill-in) resulting in optimized 50% [50%HDH] and 40% [40%HDH] hippocampal VOIs. In a subset of our study population (n = 10 controls), the choroid plexus was manually drawn on the RPM BP_{ND} image to calculate to choroid plexus / hippocampus ratio for the time window 100 to 130 min post injection. We visually assessed all PET scans and confirmed that the removed voxels showed possible overlap between the choroid plexus and hippocampus (see Fig. 1). In addition, only the eroded VOIs were partial volume corrected with HDH. This PVC method is a combination of Van Cittert iterative deconvolution (VC IDM) and HYPR denoising (HDH) (Golla et al., 2017).

2.3. Neuropsychological examination

The Mini-Mental State Examination (MMSE) was used as a measure for global cognition (Folstein et al., 1975). The Dutch translation of the Rey Auditory verbal learning (RAVLT, delayed recall condition) was used as a memory specific task, previously shown to be strongly associated with hippocampal function (Dejong, 1973; Groot et al., 2018).

In addition, to further characterize our MCI/ AD group, we assessed four cognitive domains (Groot et al., 2018), including memory (Dutch version of the Rey Auditory Verbal Learning Test immediate recall and delayed recall, Visual Association Test (VAT) version A), attention (Digit span Forward, Trial Making Test (TMT) version A, Stroop word and color naming), executive functioning (Digit span Backward, TMT version B, letter fluency test (D-A-T) and Stroop color naming) and language (VAT naming and category fluency version animals). Z-scores for the Trail Making Tests and Stroop tests were inverted so that lower scores indicated worse performance. For cognitive domain scores, we created composite scores by averaging Z scores for each individual test within a domain (with a minimum of two tests per domain).

2.4. Statistical analysis

Statistical analyses were performed using Statistical Package for the Social Sciences (SPSS, IBM version 22) and R version 3.2.2 for area under the curve (AUC) comparisons and bootstrap sensitivity analysis). Independent samples T-tests were used to calculate group differences for continuous variables between the controls and MCI/ AD patients (table 1). We performed receiver operating characteristic (ROC) area-under-the-curve (AUC) analyses to investigate which hippocampal [^{18}F]flortaucipir BP_{ND} VOI could best discriminate MCI/AD from CN. Differences in AUCs were assessed using bootstrap (n = 1000) procedures). We performed linear regressions to investigate associations between the hippocampal [^{18}F]flortaucipir BP_{ND} VOIs and delayed recall on the RAVLT or MMSE, while adjusting for age, sex and education. 95% confidence intervals were computed to test whether the relationships between [^{18}F]flortaucipir BP_{ND} and cognition overlapped or differed across VOIs.

Based on our a priori assumptions that optimizing the hippocampal VOI would result in more pronounced effects in subjects with higher hippocampal tau load or off-target [^{18}F]flortaucipir choroid plexus uptake, we performed two additional analyses. First, since higher age is associated with higher [^{18}F]flortaucipir choroid plexus binding (Johnson et al., 2016; Scholl et al., 2016), we evaluated the effect of age by performing linear regressions between [^{18}F]flortaucipir BP_{ND} VOIs and delayed recall stratified for age ($\leq$ 66.1 and $>$66.1 years, based on a median spit of the sample). This analysis was performed across the whole group and adjusted for sex and education. Second, we aimed to assess the effect of global cortical tau BP_{ND} within each diagnostic group. We therefore divided global cortical tau load in tertiles (low, medium and high) per diagnosis (CN vs. MCI/AD). These analyses were adjusted for age, sex and education.

Table 1
Clinical and demographic data.

	Total group (n = 109)	CN (n = 45)	MCI/AD(n = 64)
Age	66 ± 7	66 ± 8	66 ± 7
Sex (% female)	53 (49%)	21(47%)	32(50%)
Amyloid status (%positive)	80(73%)	16(36%)	64(100%)**
Education (Verhage score; range 1–7)	5.5 ± 1.2	5.6 ± 1.2	5.4 ± 1.1
MMSE (max 30)	25 ± 5	29 ± 1	23 ± 4**
RAVLT Delayed recall (max 15)	5.5 ± 4.5	9.5 ± 3.2	2.6 ± 2.8**
Memory domain	−2.0 ± 2.5 (n = 108)	0.1 ± 0.8(n = 44)	−3.4 ± 2.2 (n = 64)**
Executive domain	−0.5 ± 1.2 (n = 96)	0.3 ± 0.8 (n = 44)	−1.1 ± 0.1(n = 52)**
Attention domain	−0.6 ± 1.3 (n = 99)	0.2 ± 0.7(n = 45)	−1.3 ± 1.2 (n = 54)**
Language domain	−0.5 ± 1.3 (n = 96)	0.1 ± 0.7(n = 43)	−0.9 ± 0.9 (n = 53)**
BP_{ND} orig 100%	0.19 ± 0.17	0.07 ± 0.13	0.27 ± 0.15**
BP_{ND} HDH 50%	0.03 ± 0.14	−0.07 ± 0.12	0.09 ± 0.12**
BP_{ND} HDH 40%	−0.01 ± 0.13	−0.09 ± 0.11	0.05 ± 0.11**

Data is presented as mean ± SD or number (%). Education scoring is according to the Verhage (1965) system. Neuropsychological test scores were standardized into Z-scores prior to transformation into domain scores. MMSE, Mini-Mental State Examination RAVLT = Dutch version of the Rey Auditory Verbal Learning Test. AD significantly different from CN at.
**$p < 0.01$.
*$p < 0.05$.

3. Results

3.1. Participants

Demographics and clinical data are presented in Table 1. On average, participants were 66 ± 7 years, 49% female and had a MMSE score of 25 ± 5.There were no significant differences in age, education and sex between the different diagnostic groups (all $p > 0.05$). MMSE and delayed recall scores were lower for the MCI/ AD patients than cognitively normal subjects and we found higher hippocampal $BP_{ND100\%}$ in MCI/AD ($BP_{ND100\%}$= 0.27 ± 0.15) compared to cognitively normal subjects ($BP_{ND100\%}$= 0.07 ± 0.13).

3.2. MCI/ AD vs. cognitively normal subjects

All methods showed comparable discriminative effects between MCI/AD dementia and cognitively normal subjects ($AUC_{100\%}$ = 0.85[CI = 0.78–0.93]; $AUC_{50\%HDH}$ = 0.84 [CI = 0.74–0.92]; $AUC_{40\%HDH}$ = 0.83 [CI = 0.74–0.92], Fig. 2). Bootstrapping revealed no differences in AUCs between methods (all $p > 0.05$).

3.3. Associations between [^{18}F]flortaucipir hippocampal VOIs and cognition

Associations between the different hippocampal VOIs and cognition are presented in Fig. 3. Across groups, higher hippocampal [^{18}F]flortaucipir BP_{ND} was related to lower scores on MMSE (standardized betas; $\beta_{100\%}$ = −0.38[CI = −0.57−0.20]; $\beta_{50\%HDH}$ = −0.37[CI = −0.54 −0.19]; $\beta_{40\%HDH}$ = −0.35[CI = −0.53 −0.17]), delayed recall (standardized $\beta_{100\%}$ = −0.64[CI = −0.79 −0.49]; $\beta_{50\%HDH}$ = −0.61[CI = −0.76 −0.46]; $\beta_{40\%HDH}$ = −0.59[CI = −0.75 −0.44]; all $p < 0.001$)). The 95% confidence intervals overlapped across methods and thus effect sizes were considered comparable across all hippocampal VOIs (Fig. 2). Within diagnostic groups, similar results were observed across the three hippocampal VOIs (Fig. 2).

We furthermore investigated associations between the BP_{ND} in the different hippocampal VOI definitions and delayed recall across two age groups divided by median split. Associations were essentially comparable between the different methods and for the different age groups (≤ 66.1 years, $\beta_{100\%}$ = −0.72[CI = −0.92 −0.52], $\beta_{50\%}$ = −0.73 [CI = −0.94 −0.53], $\beta_{40\%}$ = −0.71[CI = −0.92 −0.50] vs. >66.1 years $\beta_{100\%}$ = −0.59[CI = −0.82 −0.36] $\beta_{50\%}$ = −0.57 [CI = −0.81 −0.34], $\beta_{40\%}$ = −0.57[CI = −0.81 −0.33]). When we further investigated associations between the different hippocampal tau VOIs and memory function for the different global cortical tau load groups, all methods showed comparable performance (see Table 2).

4. Discussion

In this study, we compared several methods to diminish spill-in effects of hippocampal [^{18}F]flortaucipir binding. A non optimized

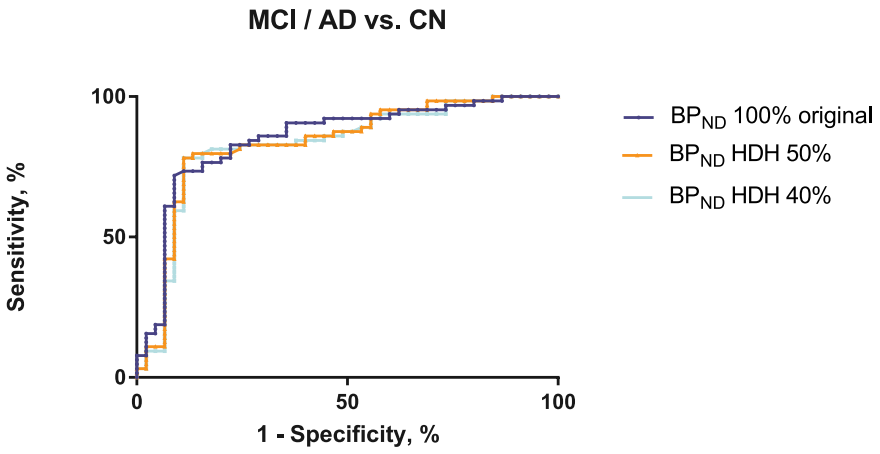

Fig. 2. Receiver operating characteristic curves of different hippocampal volume of interest (VOI) methods for distinguishing MCI/AD from CN. BP_{ND} = binding potential, HDH = Van Cittert iterative deconvolution and HYPR denoising.

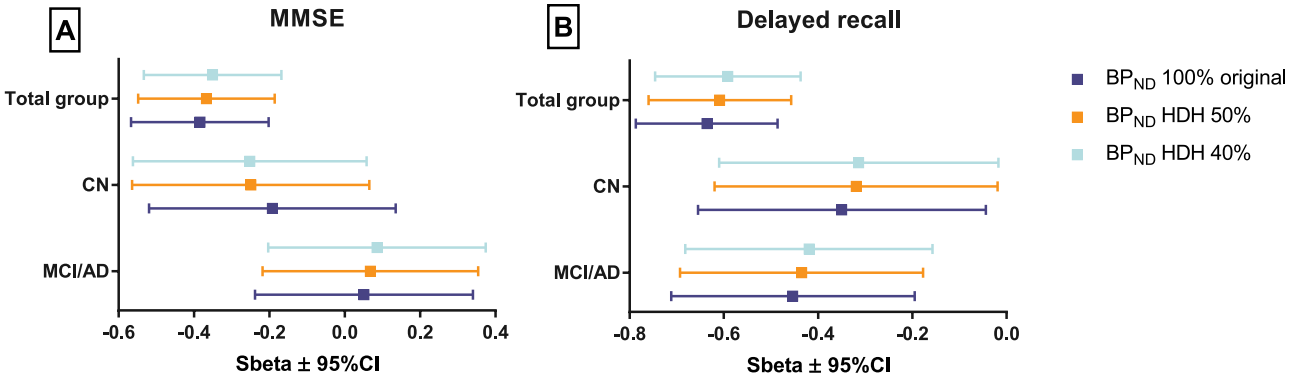

Fig. 3. Distribution of standardized Beta ± 95% confidence intervals for the association the different hippocampal VOIs between MMSE (A) and delayed recall (B) for the total group and per diagnosis.

100% hippocampal VOI ($BP_{ND100\%}$) and two additional optimized hippocampal VOIs were generated by combining Van Cittert iterative deconvolution and HYPR denoising (HDH) partial volume correction with eroding a percentage of the highest hippocampus BP_{ND} voxels (50% HDH and 40% HDH). We examined which method was able to distinguish AD from cognitively normal individuals and investigated its associations with measures of cognition. We concluded that the performance was comparable for all methods, and that after optimization the hippocampal VOIs retained strong clinico-pathological relationships.

In recent work (Wolters et al., 2018), we showed that the combination of partial volume correction (i.e. HDH) and eroding the hippocampus attenuated the relationship between hippocampal [^{18}F]flortaucipir and choroid plexus binding, indicating less spill-in from choroid plexus to neighboring hippocampus. Integrating our previous findings with the outcomes of the present study, we now show that optimization of the hippocampal tau signal leads to less spill in of the choroid plexus without the introduction of noise, since the relationship with clinical AD diagnosis and cognitive performance were comparable before and after correction.

Although the results of our previous study (Wolters et al., 2018) suggests that eroding and PVC resulted in a more accurate quantification of tau load, the isolated results of the present study show comparable results for non-optimized and optimized hippocampal VOIs. Thus non-optimized hippocampal VOIs are probably sufficient for clinical interpretation, for instance for discriminative accuracy of [^{18}F]flortaucipir between controls and MCI/AD groups or for correlational analysis of [^{18}F]flortaucipir binding with global cognitive measures such as MMSE. As such, we do not recommend use of PVC and VOI erosion for these purposes, but readers should be aware that accurate assessment of hippocampal uptake will require a proper correction for CP spillover and may be required in case of smaller effect sizes between subject groups or for longitudinal studies

In line with previous literature[6, 15], we showed that the uncorrected hippocampal VOI discriminated between AD patients and cognitively normal subjects and optimizing hippocampal tau uptake did not significantly diminish the discriminative ability. Scholl et al. (2016) showed that PVC resulted in a large increase of signal in the choroid plexus, which suggests that the spill-out of signal of the choroid plexus is decreased. Although there was an minimal change in the amount of hippocampal [^{18}F]flortaucipir tracer uptake, the PVC may ameliorate the estimation of the hippocampal [^{18}F]flortaucipir. Similar to the present study, uncorrected data also showed a clear distinction between AD patients and cognitively normal subjects and PVC data was preferred because it marginally outperformed PVC uncorrected data without altering its associations with diagnosis. In addition, Wang et al. (2016) studied two different approaches to correct for the confounding effect of the choroid plexus and concluded that after correction hippocampal tau retained its association with clinical diagnosis. While using PVC and linear regressions methods, they found a significant relationship between hippocampal and choroid plexus tau load (r = 0.39) and a significant decrease after both corrections (r = 0.14–0.19). In line with results of the current study and recent work (Wolters et al., 2018), [^{18}F]flortaucipir uptake in the hippocampus was improved after correction, while the discriminative ability of the hippocampus remained excellent and comparable with uncorrected hippocampus tau signal.

In a second approach we investigated the associations between hippocampal tau and cognitive functioning, and we found that optimization of hippocampal [^{18}F]flortaucipir binding did not alter the strong associations between tau PET and cognition. Relationships between hippocampal tau and cognition were comparable for all methods, which enhances the conclusion that the non-optimized hippocampal VOI is sufficient for clinical interpretation. This is in line with other tau PET studies, in which associations between PVC [^{18}F]flortaucipir and cognition were equivalent to the uncorrected data (Ossenkoppele et al., 2016; Scholl et al., 2016; Ossenkoppele et al., 2019). However, Lee et al.[11] examined the relationship between hippocampal tau load and cognition specifically, and showed that the adjustment of [^{18}F]flortaucipir standardized uptake value ratio (SUVr) in the hippocampus by means of partial residuals and PVC resulted in a stronger relationship with cognition. They used a combination of PVC and partial residuals of the hippocampus to correct for the choroid plexus spill in and extracted the hippocampus residuals from the univariate regression between the

Table 2
associations between the different hippocampal VOIs and delayed recall per Tau load stratified for diagnosis.

Hippocampal VOI	Cognitively normal participants (n = 45) β(95% CI)			MCI / AD (n = 64) β(95% CI)		
	Low tau load (n = 15)	Medium tau load (n = 15)	High tau load (n = 15)	Low tau load (n = 21)	Medium tau load (n = 22)	High tau load (n = 21)
100%	0.39 (−0.4–1.2)	−0.27 (−1.0–0.4)	−0.38 (−1.1–0.4)	−0.49 (−1.0–0.1)	−0.31 (−0.8–0.2)	−0.47 (−0.8–0.0)
HDH 50%	0.47 (−0.2–1.1)	−0.02 (−0.8–0.8)	−0.44 (−1.1–0.3)	−0.47 (−0.9–0.2)	−0.21 (−0.7–0.3)	−0.57 (−1.0–0.2)
HDH 40%	0.38 (−0.2–1.0)	−0.01 (−0.8–0.87)	−0.42 (−1.1–0.3)	−0.36 (−0.9–0.2)	−0.21 (−0.7–0.27)	−0.58 (−1.0–0.2)

Data is presented as standardized Beta ± 95% confidence intervals(CI) between brackets**$p<0.01$, *$p<0.05$. Analyses were adjusted for age, gender and education. Associations were calculated between hippocampal VOI and delayed recall, per diagnostic group (cognitively normal participants vs. MCI/AD) and per tau load (tertiles). Tau load was based on global BP_{ND} (VOI = volume of interest, HDH = Van Cittert iterative deconvolution and HYPR denoising).

choroid plexus and hippocampus. With the aforementioned method they showed that the adjusted hippocampal SUVr was associated with memory scores in amyloid positive participants, while unadjusted hippocampal uptake was not. A possible explanation for this discrepancy in results is that Lee et al. (2018) used SUVr. SUVr is susceptible to differences in tracer delivery between patients, i.e. dependent of the velocity of wash in and wash out of the tracer (Carson et al., 1993). Especially in AD patients (van Berckel et al., 2013), where flow effects are expected, SUVr is less reliable than BP_{ND} which was used in our study. In addition, Lee et al. used of a different PVC method, the geometric transfer matrix(GTM) (Rousset et al., 1998). GTM requires an MR image of the brain, while in our study we specifically obtained for a method in that could use a "PET only" PVC method which is less susceptible for VOI definition, registration and segmentation errors and may therefore be more accurate than MR based methods. Moreover, the study was conducted in a normal aging population, with a higher mean age (75.9 compared to 66.9 years in our cohort). As choroid plexus binding increases with age (Johnson et al., 2016; Scholl et al., 2016), adjustment of the hippocampus VOI may affect results more in the case of higher choroid plexus signal, e.g. in older age.

There are several limitations. First, we automatically eroded the hippocampus based on the voxel BP_{ND} values. The rationale for choosing this method is that the choroid plexus had much higher uptake, resulting in higher $BP_{ND,}$ than the hippocampus. To assess the extent of difference, the ratio of the uptake between the choroid plexus and hippocampus (using 100–130 min scan duration) for a subset of our study population ($n = 10$ controls) was calculated. The choroid plexus uptake was 1.6 times higher (1.1–2.7) relative to the hippocampus for visually high uptake cases. For visually low uptake cases, the choroid plexus uptake was 1.3 times higher (range 1.1–1.6) than the hippocampus. This demonstrates that the spill-in of the choroid plexus may have a high impact on the BP_{ND} of the hippocampus. The highest intensity voxels in the hippocampus would be inherently the voxels that suffer from spill-in from the choroid plexus. This is also depicted in Fig. 1, where the voxels at the hippocampus-choroid plexus border that suffer from spill-in are deleted. Since the choroid plexus has a wide anatomical variety and does not show a uniform high uptake pattern throughout the plexus, a voxel based method is presumably more accurate than a region-of-interest based method.

Second, we used cerebellar grey matter as a reference region. Our previous kinetic modelling work showed that there was no difference in the volume of distribution (V_T) values of the whole grey matter cerebellum, indicating that this is a reliable reference region for our study population (Golla et al., 2017). Another recent study of ours presented a high test-retest repeatability of [^{18}F]flortaucipir kinetics when using cerebellar gray matter as a reference region and dynamic scans, suggesting grey matter cerebellum is a reliable reference region (Timmers et al., 2019).

Third, we did not have neuropathological confirmation of the off-target binding in the choroid plexus. As suggested by others, several substrates of this off-target binding are proposed including calcification/ mineralization (Lowe et al., 2016) and leptomeningeal melanocytes (Marquie et al., 2015, 2017). The latter is confirmed by an in vivo study in which Black/African Americans showed higher flortaucipir choroid plexus binding compared to White participants, but not in other regions (Lee et al., 2018). However, some argue that part of the signal in the choroid plexus may be actually on-target, that is binding to a structure called "Biondi ring" (tau) tangles (Ikonomovic et al., 2016). This has yet to be confirmed by other post mortem studies. Fourth, the average age of our sample was relatively low. Since choroid plexus binding increases with age (Johnson et al., 2016; Scholl et al., 2016), this may have underestimated the value of partial volume correction.

In summary, among patients of a memory clinic we earlier described a reduction of the association between hippocampal and choroid plexus [^{18}F]flortaucipir retention after the combination of HDH PVC and eroding (Wolters et al., 2018). After applying and adjusting this method for clinical purposes, we showed that automated HDH 50% and 40% hippocampal [^{18}F]flortaucipir BP_{ND} retains comparable strong relationships with cognition. Although there is still a need for accurate quantitative assessment of the hippocampal [^{18}F]flortaucipir uptake, the non-optimized hippocampal VOI may be accurate enough for clinical interpretation, since both discrimination between diagnostic groups and associations between hippocampal [^{18}F]flortaucipir BP_{ND} and memory were comparable for all methods.

5. Disclosures

Wolters, Ossenkoppele, Golla, Verfaillie, Visser, Tuncel, Coomans, Windhorst, van der Flier and Boellaard report no conflict of interest.

Van der Flier received grant support from ZonMW, NWO, EU-FP7, Alzheimer Nederland, CardioVascular Onderzoek Nederland, Stichting Dioraphte, Gieskes-Strijbis Fonds, Boehringer Ingelheim, Piramal Neuroimaging, Roche BV, Janssen Stellar, Combinostics. All funding is paid to the institution. WvdF holds the Pasman chair.

Van Berckel received research support from ZON-MW, AVID radiopharmaceuticals, CTMM and Janssen Pharmaceuticals. He is a trainer for Piramal and GE. He receives no personal honoraria.

Scheltens received grant support (to the institution) from GE Healthcare, Danone Research, Piramal and MERCK. In the past 2 years he has received consultancy/speaker fees from Lilly, GE Healthcare, Novartis, Forum, Sanofi, Nutricia, Probiodrug and EIP Pharma. All funding is paid to the institution.

No other potential conflicts of interest relevant to this article exist.

CRediT authorship contribution statement

Emma E Wolters: Data curation, Formal analysis, Writing - original draft. **Rik Ossenkoppele:** Conceptualization, Visualization, Formal analysis, Data curation. **Sandeep SV Golla:** Data curation, Formal analysis, Writing - original draft. **Sander CJ Verfaillie:** Formal analysis, Data curation, Writing - original draft. **Tessa Timmers:** Data curation, Writing - review & editing. **Denise Visser:** Data curation, Writing - review & editing. **Hayel Tuncel:** Formal analysis, Data curation, Writing - review & editing. **Emma M Coomans:** Data curation, Writing - review & editing. **Albert D Windhorst:** Writing - review & editing. **Philip Scheltens:** Writing - review & editing. **Wiesje M van der Flier:** Writing - review & editing. **Ronald Boellaard:** Conceptualization, Visualization, Formal analysis, Data curation, Writing - original draft. **Bart NM van Berckel:** Conceptualization, Visualization, Formal analysis, Data curation, Writing - original draft.

Acknowledgments

The authors kindly thank all participants for their contribution. Research of Amsterdam Alzheimer Center is part of the Neurodegeneration program of Amsterdam Neuroscience. The Amsterdam Alzheimer Center is supported by Alzheimer Nederland and Stichting VUmc funds. [^{18}F]Flortaucipir PET scans were made possible by Avid Radiopharmaceuticals Inc.

References

Nelson, P.T., Braak, H., Markesbery, W.R., 2009. Neuropathology and cognitive impairment in Alzheimer disease: a complex but coherent relationship. J. Neuropathol. Exp. Neurol. 68 (1), 1–14.

Braak, H., Braak, E., 1991. Neuropathological stageing of Alzheimer-related changes. Acta Neuropathol. 82, 239–259.

Ossenkoppele, R., et al., 2016. Tau PET patterns mirror clinical and neuroanatomical variability in Alzheimer's disease. Brain 139 (Pt 5), 1551–1567.

Johnson, K.A., et al., 2016. Tau positron emission tomographic imaging in aging and early Alzheimer disease. Ann. Neurol. 79 (1), 110–119.

Scholl, M., et al., 2016. PET imaging of Tau deposition in the aging human brain. Neuron 89 (5), 971–982.

Pontecorvo, M.J., et al., 2017. Relationships between flortaucipir PET Tau binding and

amyloid burden, clinical diagnosis, age and cognition. Brain 140 (3), 748–763.
Ossenkoppele, R., et al., 2018. Discriminative accuracy of [18F]flortaucipir positron emission tomography for Alzheimer disease vs other neurodegenerative disorders. JAMA 320 (11), 1151–1162.
Vermeiren, C., et al., 2018. The Tau positron-emission tomography tracer AV-1451 binds with similar affinities to Tau fibrils and monoamine oxidases. Mov. Disord. 33 (2), 273–281.
Lowe, V.J., et al., 2016. An autoradiographic evaluation of AV-1451 Tau PET in dementia. Acta Neuropathol. Commun. 4 (1), 58.
Lee, C.M., et al., 2018. 18F-Flortaucipir Binding in choroid plexus: related to race and hippocampus signal. J. Alzheimers Dis. 62 (4), 1691–1702.
Wang, L., et al., 2016a. Evaluation of Tau imaging in staging Alzheimer disease and revealing interactions between beta-Amyloid and tauopathy. JAMA Neurol. 73 (9), 1070–1077.
Wolters, E.E., et al., 2018. A novel partial volume correction method for accurate quantification of [(18)F] flortaucipir in the hippocampus. EJNMMI Res. 8 (1), 79.
Price, J.L., Morris, J.C., 1999. Tangles and plaques in nondemented aging and "preclinical" Alzheimer's disease. Ann. Neurol. 45 (3), 358–368.
Wang, L., et al., 2016b. Evaluation of Tau imaging in staging Alzheimer disease and revealing interactions between beta-amyloid and Tauopathy. JAMA Neurol. 73 (9), 1070–1077.
Golla, S.S.V., et al., 2017a. Partial volume correction of brain PET studies using iterative deconvolution in combination with HYPR denoising. EJNMMI Res. 7 (1), 36.
Slot, R.E.R., et al., 2018. Subjective cognitive impairment cohort (SCIENCe): study design and first results. Alzheimers Res. Ther. 10 (1), 76.
van der Flier, W.M., et al., 2014. Optimizing patient care and research: the Amsterdam dementia cohort. J. Alzheimers Dis. 41 (1), 313–327.
van der Flier, W.M., Scheltens, P., Amsterdam Dementia Cohort, 2018. Performing research to optimize care. J. Alzheimers Dis. 62 (3), 1091–1111.
Albert, M.S., et al., 2011. The diagnosis of mild cognitive impairment due to Alzheimer's disease: recommendations from the national institute on aging-Alzheimer's association workgroups on diagnostic guidelines for Alzheimer's disease. Alzheimers Dement. 7, 270–279.
McKhann, G.M., et al., 2011. The diagnosis of dementia due to Alzheimer's disease: recommendations from the national institute on aging-alzheimer's association workgroups on diagnostic guidelines for Alzheimer's disease. Alzheimers Dement. 7, 263–269.
Seibyl, J., et al., 2016. Impact of training method on the robustness of the visual assessment of 18F-Florbetaben PET scans: results from a phase-3 study. J. Nucl. Med. 57 (6), 900–906.
Zwan, M., et al., 2014. Concordance between cerebrospinal fluid biomarkers and [11C] PIB PET in a memory clinic cohort. J. Alzheimers Dis. 41, 801–807.
Tijms, B.M., et al., 2018. Unbiased approach to counteract upward drift in cerebrospinal fluid amyloid-beta 1-42 analysis results. Clin. Chem. 64 (3), 576–585.
Golla, S.S., et al., 2018a. Quantification of [(18)F]florbetapir: a test-retest tracer kinetic modelling study. J. Cereb. Blood Flow Metab., 271678×18783628.
Golla, S.S.V., et al., 2017b. Quantification of Tau load using [18F]AV1451 PET. Mol. Imaging Biol. 19 (6), 963–971.
Vollmar, S., et al., 2002. HeinzelCluster: accelerated reconstruction for fore and osem3d. Phys. Med. Biol. 47 (15), 2651–2658.
Hammers, A., et al., 2003. Three-dimensional maximum probability atlas of the human brain, with particular reference to the temporal lobe. Hum. Brain Mapp. 19 (4), 224–247.
Svarer, C., et al., 2005. MR-based automatic delineation of volumes of interest in human brain PET images using probability maps. Neuroimage 24 (4), 969–979.
Golla, S.S., et al., 2018b. Parametric methods for [(18)F]flortaucipir PET. J. Cereb. Blood Flow Metab., 271678×18820765.
Timmers, T., et al., 2019. Test-retest repeatability of [(18)F]Flortaucipir PET in Alzheimer's disease and cognitively normal individuals. J. Cereb. Blood Flow Metab., 271678×19879226.
Folstein, M.F., Folstein, S.E., McHugh, P.R., 1975. Mini-mental state". a practical method for grading the cognitive state of patients for the clinician. J. Psychiatr. Res. 12, 189–198.
Dejong, R.N., 1973. Hippocampus and its role in memory - clinical manifestations and theoretical considerations. J. Neurol. Sci. 19 (1), 73–83.
Groot, C., et al., 2018a. Clinical phenotype, atrophy, and small vessel disease in APOEepsilon2 carriers with Alzheimer disease. Neurology 91 (20), e1851–e1859.
Groot, C., et al., 2018b. Differential effects of cognitive reserve and brain reserve on cognition in Alzheimer disease. Neurology 90 (2), e149–e156.
Ossenkoppele, R., et al., 2019. Associations between Tau, abeta, and cortical thickness with cognition in Alzheimer disease. Neurology 92 (6), e601–e612.
Carson, R.E., et al., 1993. Comparison of bolus and infusion methods for receptor quantitation: application to [18F]cyclofoxy and positron emission tomography. J. Cereb. Blood Flow Metab. 13 (1), 24–42.
van Berckel, B.N., et al., 2013. Longitudinal amyloid imaging using 11C-PiB: methodologic considerations. J. Nucl. Med. 54 (9), 1570–1576.
Rousset, O.G., Ma, Y., Evans, A.C., 1998. Correction for partial volume effects in PET: principle and validation. J. Nucl. Med. 39 (5), 904–911.
Marquie, M., et al., 2015. Validating novel Tau PET tracer [F-18]-AV-1451 (T807) on postmortem brain tissue. Ann. Neurol. 78 (5), 787–800. https://doi.org/10.1002/ana.24517.
Marquie, M., et al., 2017. Lessons learned about [F-18]-AV-1451 off-target binding from an autopsy-confirmed Parkinson's case. Acta Neuropathol. Commun. 5 (1), 75.
Ikonomovic, M.D., et al., 2016. [F-18]AV-1451 positron emission tomography retention in choroid plexus: more than "off-target" binding. Ann. Neurol. 80 (2), 307–308.